Conference Paper, Published Version

Shao, Songdong; Tait, Simon

Incompressible SPH Simulation of Solitary Wave Generation and Run-Up Due to Boundary Movement

Verfügbar unter/Available at: https://hdl.handle.net/20.500.11970/110089

Vorgeschlagene Zitierweise/Suggested citation:
Shao, Songdong; Tait, Simon (2008): Incompressible SPH Simulation of Solitary Wave Generation and Run-Up Due to Boundary Movement. In: Wang, Sam S. Y. (Hg.): ICHE 2008. Proceedings of the 8th International Conference on Hydro-Science and Engineering, September 9-12, 2008, Nagoya, Japan. Nagoya: Nagoya Hydraulic Research Institute for River Basin Management.

INCOMPRESSIBLE SPH SIMULATION OF SOLITARY WAVE GENERATION AND RUN-UP DUE TO BOUNDARY MOVEMENT

Songdong Shao[1] and Simon Tait[2]

[1] Lecturer in Environmental Fluid Mechanics, School of Engineering, Design and Technology, University of Bradford, West Yorkshire, BD7 1DP, UK, e-mail: s.shao@bradford.ac.uk
[2] Professor in Civil Engineering, School of Engineering, Design and Technology, University of Bradford, West Yorkshire, BD7 1DP, UK, e-mail: s.tait@bradford.ac.uk

ABSTRACT

The Smoothed Particle Hydrodynamics (SPH) method is a mesh-free particle modelling approach which is capable of treating free surfaces and the motion of solid boundaries in a straightforward, but accurate way. The incompressible SPH model (IncomSPH) in the paper is different from the traditional weakly compressible SPH approach, as it employs a strict incompressible hydrodynamic formulation to solve the pressures and the solution process is based on a two-step split schemes of predictor and corrector. A moving boundary is used to generate the solitary wave and is described by using “mirror” particles to satisfy strictly the boundary conditions. IncomSPH is used to simulate the generation and run-up of a solitary wave. The propagation and run-up processes are computed and compared with the experimental data and numerical results from the Shallow Water Equation (SWE) model and good agreement is generally found. Finally, the wave characteristics in the surf zone are illustrated and the model limitations are discussed.

Keywords: incompressible, SPH, solitary wave, boundary movement, turbulence

1. INTRODUCTION

Upon reaching the shoreline, tsunami waves can break and travel inland for large distances with the potential for large amounts of property damage and loss of life. Being able to predict this process is therefore an important pre-requisite of any mitigation effort. Solitary wave or combinations of negative and positive solitary-like waves are often used to simulate the run-up and shoreward inundation. The study of solitary wave generation, run-up and breaking has therefore both theoretical interest and practical significance.

Numerous experimental and numerical studies have been made to investigate the generation and run-up of the solitary waves. Monaghan and Kos (1999) experimentally generated a solitary wave by dropping a heavy box from above the water surface and simulated its propagation over shallow water and its return back after being reflected from a vertical wall using the weakly compressible Smoothed Particle Hydrodynamics approach. Guizien and Barthelemy (2002) used a new experimental procedure to generate solitary waves in a wave flume using a piston type wave-maker based on the Rayleigh's solitary wave solution, and compared their observations with the solitary waves generated by the Boussinesq, first-order KdV and second-order shallow water theories. Liu et al. (2006) performed a set of laboratory experiments to measure the viscous damping and shoaling of a solitary wave propagating in a wave tank and compared it with numerical solutions from a 2-D depth-averaged Boussinesq-type equation.

Tsunami waves or solitary waves are long waves, so the Shallow Water Equation (SWE) model has been widely used to perform numerical simulations of this type of wave with great

CPU efficiency. However, the SWE is based on the depth-average and hydrostatic assumptions, so it can not be expected to provide an accurate solution where the vertical acceleration or velocity is large. Cea et al. (2004) used three different wave paddles to generate solitary waves and investigated their propagations and run up over a variety of water depths and topographies. The experimental data compared well with the numerical results obtained from the SWE model based on a finite volume approach. They further investigated the influence of turbulence modelling and treatment of wet-dry boundaries as well as the limitations of the SWE model.

The Smoothed Particle Hydrodynamics (SPH) method (Monaghan, 1992) was first originated in astrophysics for the study of the fluid dynamics of interstellar gas and later extended to model a wide range of hydrodynamics problems. SPH is a fully Lagrangian approach in which the particles move in Lagrangian coordinates and the advection term in hydrodynamic equations (Navier-Stokes equations) is directly calculated by the particle motion without numerical diffusion. So the SPH model can accurately describe free surfaces and moving boundaries. In this paper, an incompressible version of the SPH model (Lo and Shao, 2002) is applied to simulate the whole processes of the generation of a solitary wave by the motion of a wave paddle, the wave propagation and running-up over a slope based on the experimental conditions of Cea et al. (2004). The incompressible SPH computations are also compared with the numerical results from a SWE model of Cea et al. (2004). Finally, the wave characteristics in the surf zone are discussed and a comparison is also made with regard to the SPH and SWE numerical models.

2. INCOMPRESSIBLE SPH MODEL (IncomSPH)

The IncomSPH code solves the following Lagrangian form of hydrodynamic equations by using an SPH formulation:

$$\frac{1}{\rho}\frac{d\rho}{dt} + \nabla \cdot \mathbf{u} = 0 \tag{1}$$

$$\frac{d\mathbf{u}}{dt} = -\frac{1}{\rho}\nabla P + \mathbf{g} + \nu_0 \nabla^2 \mathbf{u} + \frac{1}{\rho}\nabla \cdot \overset{\Rightarrow}{\boldsymbol{\tau}} \tag{2}$$

where ρ = fluid density; t = time; $\mathbf{u}$ = velocity; P = pressure; $\mathbf{g}$ = gravitational acceleration; ν_0 = kinematic viscosity and $\overset{\Rightarrow}{\boldsymbol{\tau}}$ = turbulence stress, which is treated by using a Smagorinsky model in IncomSPH.

In the SPH concept, the motion of each particle is calculated through the interactions with its neighbouring particles using an analytical kernel function. All terms in the governing equations can be represented by particle interaction models and thus a grid is not needed. The standard SPH formulations are used to treat each term in the Equations (1) and (2), including the SPH summation, density and gradient and divergence operators. The spline-based kernel function normalized in 2-D is used for these operators. However, the second-order operators of viscosity and Laplacian are formulated in the IncomSPH by a hybrid of a standard SPH divergence with a first-order finite difference to ensure numerical stability (Lo and Shao, 2002).

In IncomSPH computations, the governing Equations (1) and (2) are solved through a two-step prediction-correction process. The prediction step is an explicit integration in time without enforcing the incompressibility, i.e., only the gravitational forces, the viscous and turbulent stresses in Equation (2) are used and an intermediate particle velocity and position are obtained. At this stage, the incompressibility of the fluids is violated due to the particle motion, which is manifested by the deviations of the intermediate particle density ρ_* from the initial density ρ_0. In order to satisfy the incompressibility requirement, the pressure is used to update the intermediate particle velocity and position in the correction step. A unique feature of the IncomSPH model lies in that the pressure is calculated from a pressure Poisson equation derived from the mass and momentum equations as:

$$\nabla \cdot \left(\frac{1}{\rho_*}\nabla P\right) = \frac{\rho_0 - \rho_*}{\rho_0 \Delta t^2} \tag{3}$$

This semi-implicit algorithm of calculating the pressures distinguishes the IncomSPH from the weakly compressible SPH approach (Monaghan, 1992), in which the pressure is determined by a thermodynamic equation.

3. NUMERICAL TREATMENT OF FREE SURFACES AND SOLID BOUNDARIES

In the SPH computations, free surfaces can be easily and accurately tracked by the location of the particles. Since there are no particles above the free surface, the particle density abruptly drops at the free surface location. A zero pressure is given to each of the surface particles and thus the surface particles are not involved in the solution process of the pressure Poisson equation.

The fixed solid boundaries such as the bottom and slope walls are treated by fixed wall particles, which balance the pressure of inner fluid particles and prevent them from penetrating the wall. The pressure Poisson equation should be solved on the wall particles in the IncomSPH computations, a process which is very similar to the pressure projection approach widely used in the grid method (Chorin, 1968).

The wave generating boundary is also modelled by a group of wall particles but they are not fixed in space. In the computations, these particles are moved in the same way as a physical wave paddle used in the laboratory experiment. In order to better satisfy the boundary conditions here, the mirror particle approach is used to treat the wave generating boundary (Lo and Shao, 2002). As shown in Figure 1, with regard to the interaction between an inner fluid particle a and b, an additional interaction between a and a mirror b_{mir} is included if a and b are close to a wall. The position of b_{mir} is set by a direct reflection of particle b across the boundary. The velocity of b_{mir} is set to be opposite of that of particle b for a non-slip boundary, i.e. $\mathbf{u}_{b,mirror} = -\mathbf{u}_b$. The pressure of b_{mir} is equal to the pressure of particle b. Thus the homogeneous Neumann boundary condition $\partial P / \partial n = 0$ is enforced.

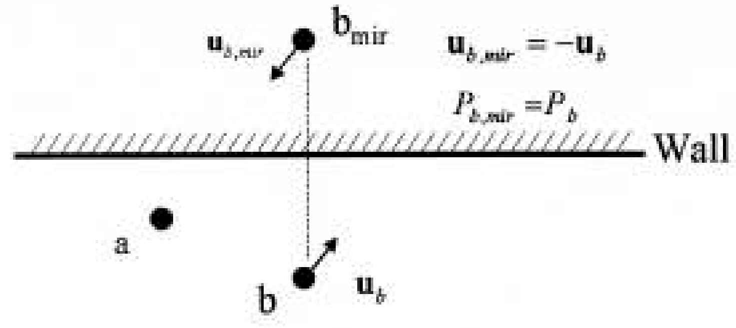

Figure 1 Wave generating boundary by mirror particles (Lo and Shao, 2002)

4. MODEL APPLICATIONS

The IncomSPH model is applied to generate a solitary wave based on the laboratory experiments of Cea et al. (2004). The experiments were carried out in a 0.60 m wide and 15 m long wave flume. The solitary waves were generated by the horizontal movement of a wave paddle which was located at the entrance to the flume. Detailed measurements were made to record the water surface elevations at several locations along the flume. A wide range of experimental conditions were used with the still water depth ranging from 0.15 m to 0.40 m. The wave paddles with three different slopes 45°, 60° and 90° were moved with a slow velocity of 0.29 m/s and a fast velocity of 0.58 m/s, respectively. The IncomSPH model is used to reproduce the experiment in which the solitary wave was generated by a vertical paddle to run up a 0.16 slope with the initial water depth of 0.40 m.

In the IncomSPH computations, the computational domain is 6 m long covering a domain with 3 m long flat bottom and 3 m slope, as compared with 15 m long domain in the physical experiment. The focus of study is the wave breaking and running-up processes in the surf zone. By balancing the computational efficiency and accuracy, an initial particle spacing of 0.02 m is used in the SPH simulation. The particle spacing is consistent with the grid spacing 0.024 m used by Cea et al. (2004) in the Shallow Water Equation (SWE) modelling, so the comparisons of the two numerical results can be made on an objective basis. The wave paddle is moved with a uniform velocity of 0.29 m/s for 2 seconds and then stopped without returning to its original position. Thus a numerical solitary wave forms and propagates along the flume and slope in the same way as that in the laboratory experiments. A sketch of the numerical wave flume and measurement positions is shown in Figure 2.

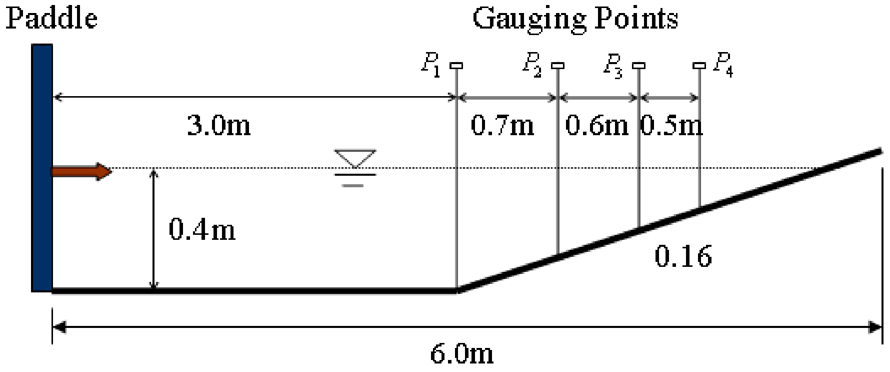

Figure 2 Sketch of numerical wave flume and measurement stations

Based on the SPH simulations, particle snapshots and velocity fields are shown in Figures 3 (a) and (b) and 4 (a) and (b), respectively. It shows the solitary wave running up and overtopping on the slope. The velocity fields further indicate that the maximum velocities always occur at the wave front. At time $t = 4.8$ s, although the wave front still continues to overtop on the slope crest, the lower part of the wave front has already begun to retreat and the water flows down the slope due to gravity. The general features of the simulation are observed to be very similar to those reported by Cea et al. (2004) in the laboratory experiments and their SWE simulations.

To investigate the influence of turbulence during this process, the turbulence model in the IncomSPH is deactivated and the model is re-run. The particle snapshots and velocity fields at the same times are shown in Figures 5 (a) and (b) and 6 (a) and (b), respectively. Compared with Figures 3 and 4, it is shown that little difference is observed between the two SPH runs with and without the modelling of turbulence. The same conclusion was also obtained by Cea et al. (2004). The reason is caused by the fact that the solitary wave actually breaks and runs up over a generally steep slope of 0.16 in the experiment. Under such conditions, the wave reflection effect is more predominant than the wave breaking effect and thus the generation of turbulence in the surf zone is relatively weak. The generation of strong turbulence should therefore be related to severe wave breaking when the slope is milder.

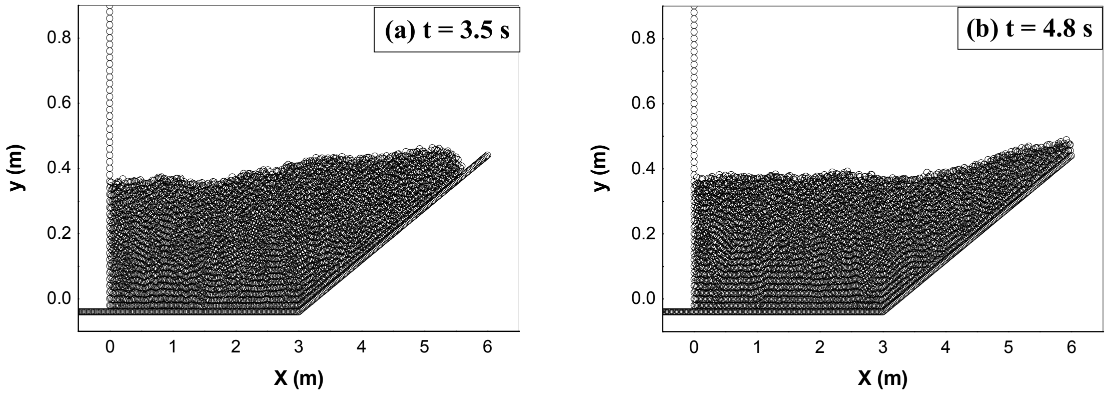

Figure 3 (a) and (b) Particle snapshots during solitary wave propagation and running up the slope

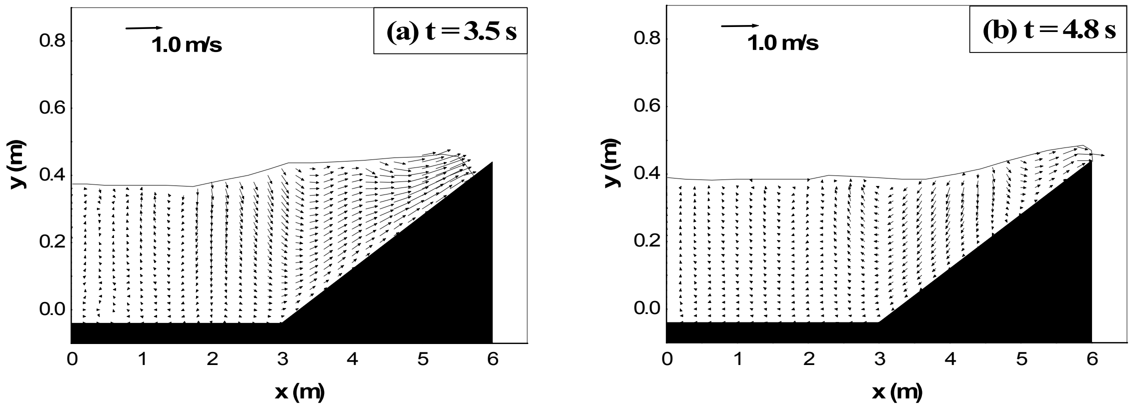

Figure 4 (a) and (b) Velocity fields during solitary wave propagation and running up the slope

A quantitative comparison of the wave profiles is shown in Figure 7 (a) and (b), based on the IncomSPH computations with and without the turbulence modelling, and the numerical results from the SWE model and the experimental data of Cea et al. (2004). A generally good agreement is shown and the maximum error between SPH results and experimental data is within 10% of the water depth. However, it should be noted that the SPH computation without the modelling of turbulence seems to match the experimental data better than the computation with the modelling of turbulence. Besides, there still exist discrepancies (20% of the water depth) between the numerical results of SPH and SWE (Cea et al. 2004) over the slope. This is caused by the SWE model being based on hydrostatic theory and therefore the vertical velocities and accelerations of the fluid particles are ignored. Besides, there are particle fluctuations in the SPH computations which also influence the accuracy.

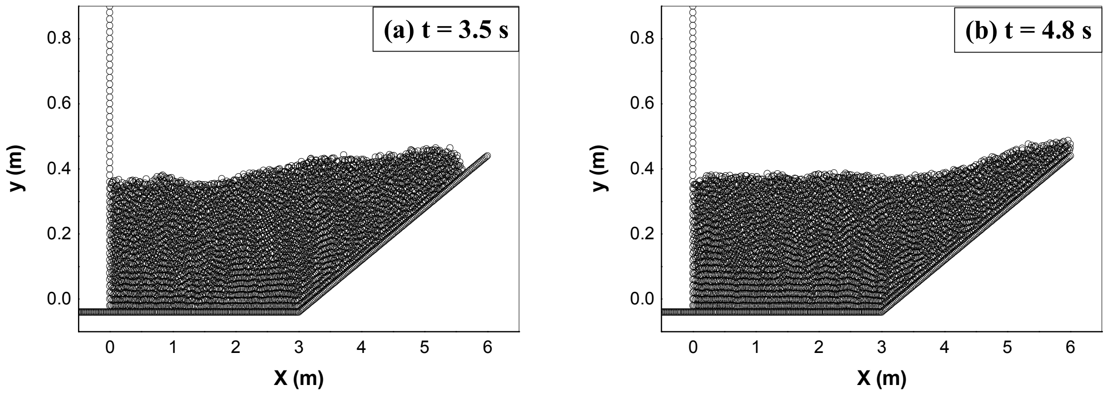

Figure 5 (a) and (b) Particle snapshots during solitary wave propagation and running up the slope computed without modelling of turbulence

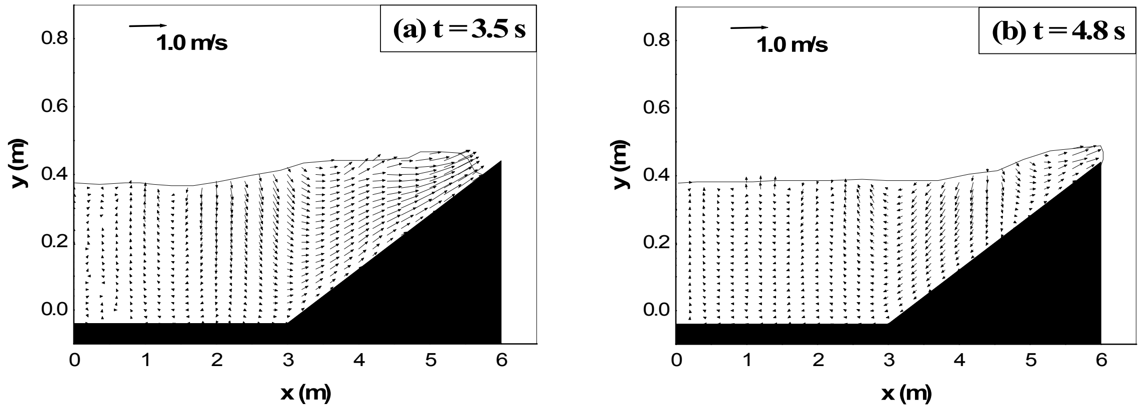

Figure 6 (a) and (b) Velocity fields during solitary wave propagation and running up the slope computed without modelling of turbulence

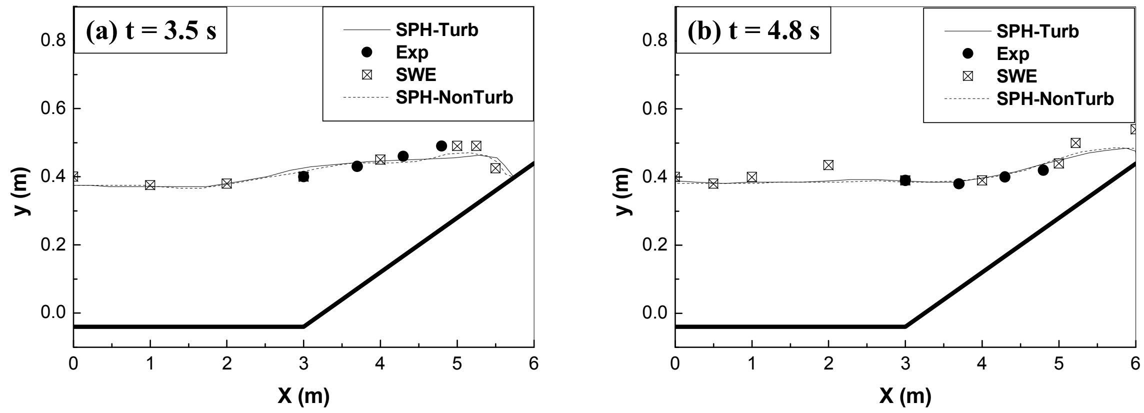

Figure 7 (a) and (b) Comparison of wave profiles computed by IncomSPH with and without modelling of turbulence and computed by SWE model and experimental data of Cea et al. (2004)

A detailed comparison of the time history of the water surfaces is shown in Figure 8 (a) and (b), based on the IncomSPH computations with and without the turbulence modeling and the SWE computations of Cea et al. (2004). The numerical results are presented for the water surface levels at the last two gauging stations P_3 and P_4. In Figure 8, the vertical coordinate has been shifted from that in the original paper of Cea et al. (2004) so as to be consistent with the still water depth of 0.4 m. However, the experimental data is not available for a comparison as the original figure resolution in Cea et al. (2004) was not clear enough.

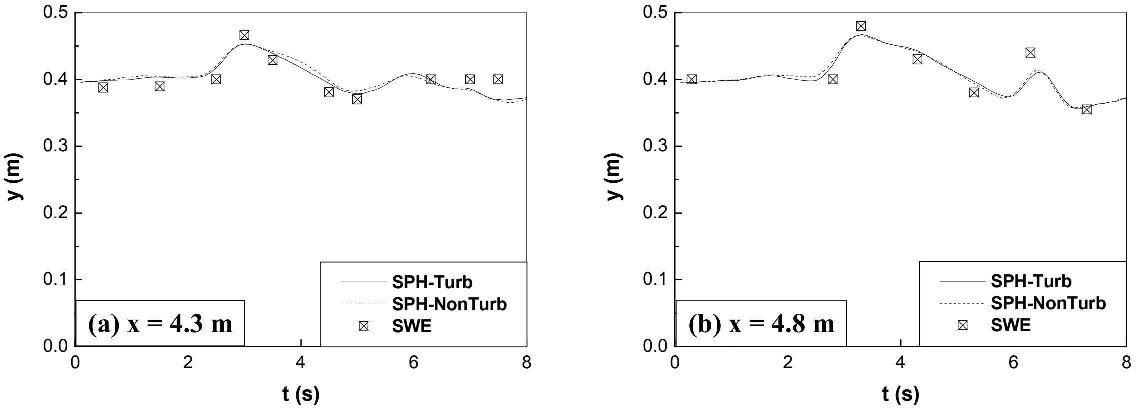

Figure 8 (a) and (b) Comparison of water surface time histories at two gauging stations P_3 and P_4, computed by SWE model of Cea et al. (2004) and IncomSPH with and without modelling of turbulence

It is shown that the agreement between two model predictions is satisfactory (the maximum deviation is within 8% of the water depth) and both numerical models can reasonably detect the high frequency oscillations in the time history of water surfaces. There is no significant difference between the two SPH runs with and without the turbulence modeling, which implies that the generation of turbulence is not significant in this application. However, the SPH computations seem to under-predict the wave amplitude more than the SWE results. As mentioned previously, the SWE model is based on the hydrostatic theory and the vertical velocities and accelerations of fluid particles are ignored. Therefore, the SWE model can not be expected to provide a good prediction over a slope of 0.16 where the vertical effects can not be neglected. On the other hand, although no assumption is introduced in the SPH model, it is inherent in the use of a particle model that the slight fluctuations of fluid particles are inevitable arising from the particle interactions and motions. As a result, there is also a corresponding fluctuation of the water surface. Usually the fluctuation of the water surface is of the order of particle spacing, which is 0.02 m in this computation. Methods to separate the particle fluctuations and high frequency water surface oscillations during the wave-structure interactions are the subject of further investigations.

5. CONCLUSIONS

The paper presents the IncomSPH model and shows it is able to simulate solitary wave generation and run-up over a slope. The simulations are in good agreement with previous experimental data and numerical results from an SWE model and the maximum error is within 10%. The SPH model is very efficient as it treats the free surface and the motion of physical boundaries in a straightforward way. The computations finished within 30 minutes by using a CPU 2.13 G and RAM 1.0 G Laptop. The model used 5000 particles and ran for 2000 steps in a 10 seconds wave simulation. The computations disclose that the turbulence generation is relatively weak for a wave breaking over a steeper slope and the problem can be reasonably solved by a numerical model without the modelling of turbulence. The study also revealed the existence of high frequency oscillations in the water surface due to the interactions between the waves and the structure. Additional work is needed to separate the fluctuations of fluid particles from the high frequency of water surface oscillations. This could lead to more accurate predictions of the history of water surfaces with highly nonlinear effects.

ACKNOWLEDGMENTS

The first author is very grateful to Professor Hitoshi Gotoh at Kyoto University and Professor Seiichi Koshizuka at the University of Tokyo, for their invaluable guidance on the incompressible SPH modelling when the author was working as JSPS fellow in Japan.

REFERENCES

Cea, L., Ferreiro, A., Vazquez-Cendon, M. E., Puertas, J. (2004), Experimental and numerical analysis of solitary waves generated by bed and boundary movements, *International Journal for Numerical Methods in Fluids,* 46, pp.793-813.

Chorin, A. J. (1968), Numerical solution of the Navier-Stokes equations, *Mathematical Computation*, 22, pp.745-762.

Guizien, K., Barthelemy, E. (2002), Accuracy of solitary wave generation by a piston wave maker, *Journal of Hydraulic Research*, 40(3), pp.321-331.

Liu, P. L. F., Simarro, G., Vandever, J., Orfila, A. (2006), Experimental and numerical investigation of viscous effects on solitary wave propagation in a wave tank, *Coastal Engineering,* 53 (2-3), pp.181-190.

Lo, E. Y. M., Shao, S. D. (2002), Simulation of near-shore solitary wave mechanics by an incompressible SPH method, *Applied Ocean Research*, 24(5), pp.275-286.

Monaghan, J. J. (1992), Smoothed particle hydrodynamics, *Annual Review of Astronomy and Astrophysics*, 30, pp.543-574.

Monaghan, J. J., Kos, A. (1999), Solitary waves on a cretan beach, *Journal of Waterway, Port, Coastal and Ocean Engineering, ASCE*, 125(3), pp.145-155.